Application Note 82:
Real-Time Detection of Peptide Aggregation During SPPS

Produced by Vapourtec

Introduction

Peptide aggregation remains one of the most significant challenges in solid-phase peptide synthesis (SPPS), often leading to incomplete coupling, reduced crude purity, and difficulties during scale-up. These effects are particularly pronounced in sequences prone to β-sheet formation or containing extended hydrophobic regions, where aggregation of the growing peptide chain restricts reagent access and reduces reaction efficiency. Despite its importance, peptide aggregation is usually inferred indirectly from declining coupling efficiencies or poor final product quality, making it difficult to identify precisely when and where aggregation occurs during a synthesis.

For more details, please contact:
Vapourtec Application Support
application.support@vapourtec.com or call:
+44 (0) 1284 728659

This application note presents seven representative peptide sequences—six known to exhibit aggregation and one non-aggregating control—analyzed using the Vapourtec Peptide-Builder™. By continuously monitoring resin volume with the patented Variable Bed Flow Reactor (VBFR™), aggregation events can be observed in real time and correlated directly with individual amino acid coupling and deprotection steps.

The results are presented as intuitive bar charts, providing a clear and quantitative visualisation of both the location and severity of aggregation throughout each synthesis. These data demonstrate how real-time VBFR™ analysis can improve understanding of peptide behaviour, facilitate troubleshooting of difficult sequences, and support the optimization of challenging peptide syntheses.

Background

Throughout the synthesis, the Vapourtec software continuously analyses VBFR™ resin volume measurements and displays the results as bar charts, enabling aggregation events to be visualised and precisely localised within the peptide sequence. The data is presented in two complementary formats. The example charts below, from the synthesis of a 30-mer GLP-1 analogue, explain how to interpret each format before examining examples of peptide aggregation.

The first visualisation is a cumulative bar chart showing how the peptidyl resin volume changes throughout the synthesis. Under normal conditions, each coupling results in a progressive increase in resin volume as the peptide chain elongates. Peptide aggregation is identified as a reduction in, or deviation from, this expected trend. In this example, a distinct aggregation event is observed at coupling 10.

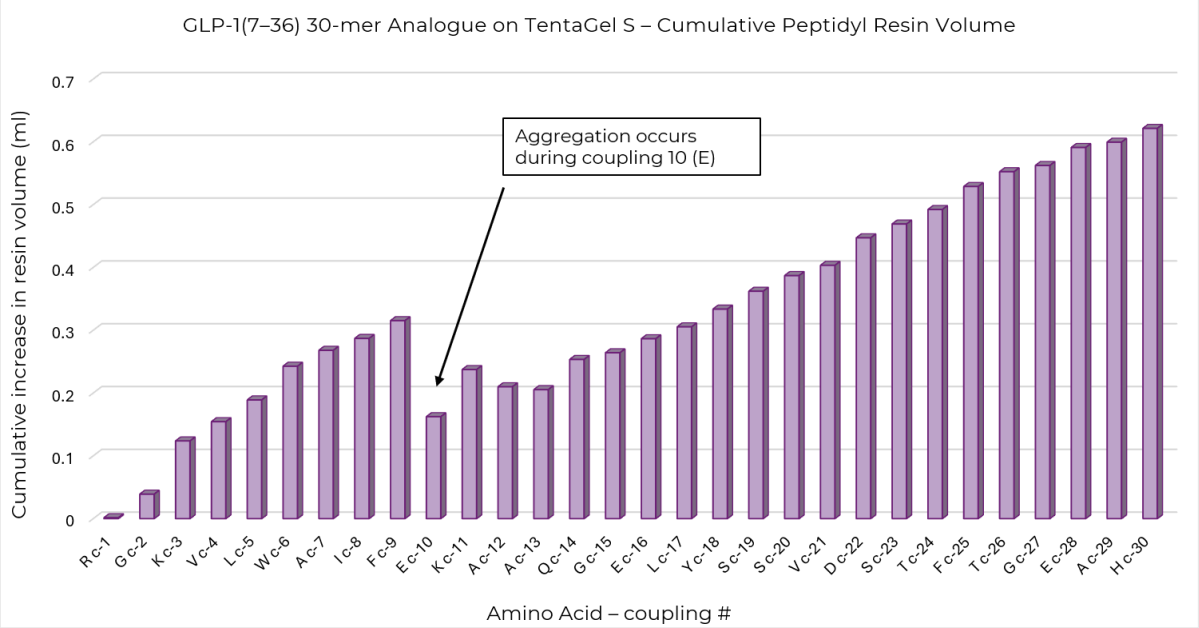

The second visualisation provides higher-resolution insight into the timing of aggregation. Each bar represents a single amino acid residue, with the coupling and deprotection phases displayed separately (coupling in solid orange, deprotection outlined). By separating these two stages, users can determine whether aggregation develops during coupling, deprotection, or both, providing valuable insight into the behaviour of individual peptide sequences. In the GLP-1 example below, the data clearly show that aggregation occurs during the coupling of glutamic acid (E), rather than during the subsequent deprotection step.

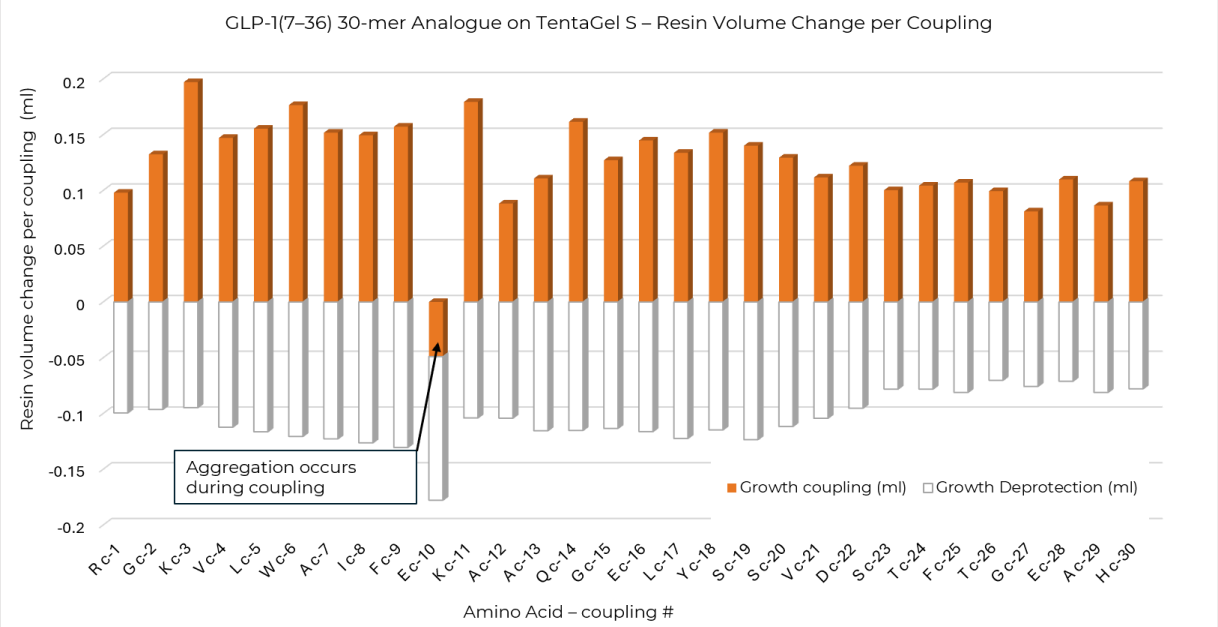

Results

To demonstrate the capability of VBFR™ analysis across a range of peptide chemistries, seven representative sequences were synthesized under standard Fast-Flow SPPS conditions. These included a non-aggregating control together with six sequences known to exhibit varying degrees of on-resin aggregation.

- 30-mer non-aggregating control peptide on TentaGel S
- JR-10 peptide on TentaGel S (aggregation-prone model peptide)
- JR-10 peptide on low-loading polystyrene resin
- ACP peptide on TentaGel S (all couplings in DMF)
- ACP peptide on TentaGel S (DMSO added for the final coupling)
- GLP-1 analogue 30-mer on TentaGel S
- Barstar fragment on TentaGel S

The examples progress from a non-aggregating control to increasingly challenging peptide syntheses, illustrating how VBFR™ analysis identifies the onset, severity and progression of aggregation under different synthesis conditions.

30-mer Non-Aggregating Control Peptide

The first example is the IGF-1(41–70) 30-mer fragment, corresponding to the C-terminal region of human insulin-like growth factor 1 (IGF-1). This sequence contains a balanced distribution of hydrophobic and hydrophilic amino acid residues and does not undergo aggregation during synthesis. In the absence of aggregation, the peptidyl resin volume increases steadily as each amino acid is coupled, producing a smooth cumulative profile. This behaviour would be expected to continue throughout the synthesis of much longer peptides, including sequences exceeding 100 amino acids in length.

The second bar chart shows the change in peptidyl resin volume for each individual coupling and deprotection step. For a non-aggregating peptide, the increase in resin volume during each coupling and the corresponding decrease during each deprotection are highly consistent from one residue to the next. This characteristic pattern provides a useful baseline against which aggregation events in more challenging peptide sequences can be readily identified.

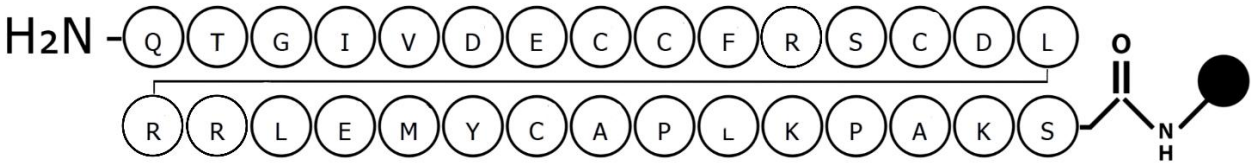

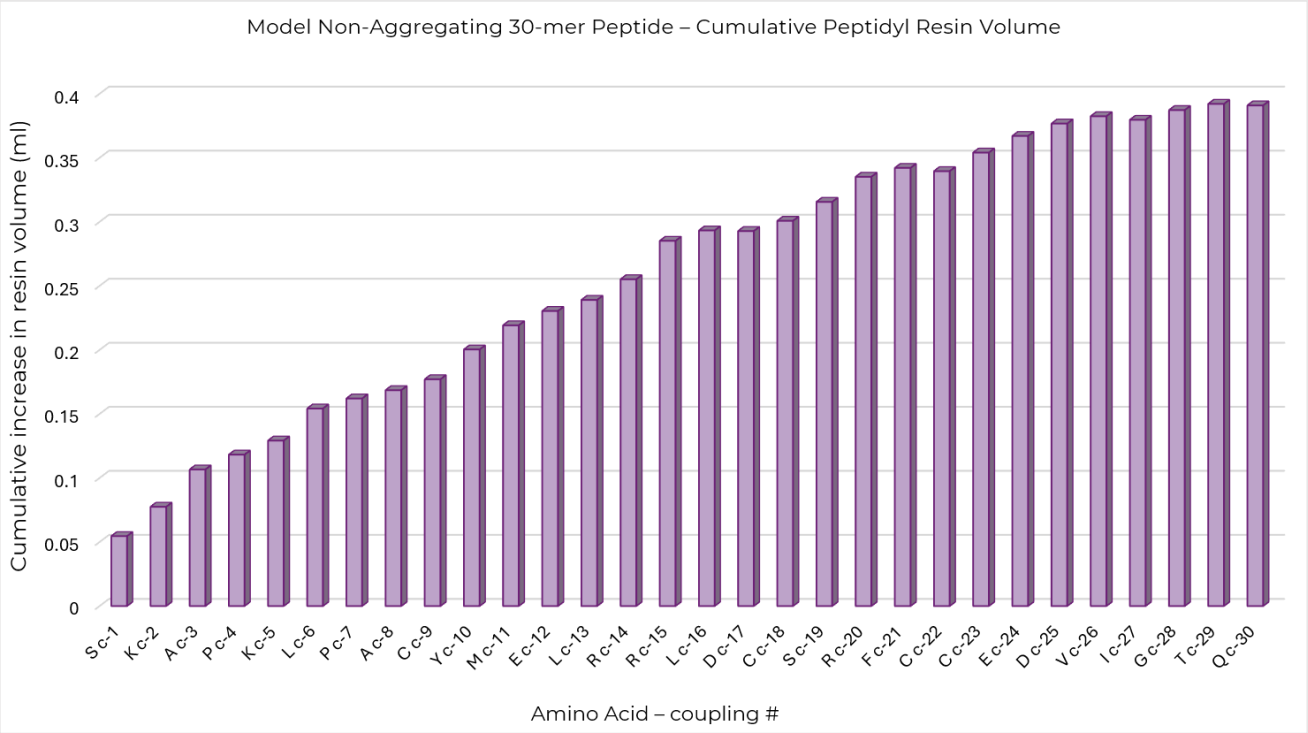
Model Non-Aggregating 30-mer Peptide – Cumulative Peptidyl Resin Volume
Cumulative increase in resin volume (ml)
0.4
0.35
0.3
0.25
0.2
0.15
0.1
0.05
0
Sc-1 Kc-2 Ac-3 Pc-4 Kc-5 Lc-6 Pc-7 Ac-8 Cc-9 Yc-10 Mc-11 Ec-12 Lc-13 Rc-14 Rc-15 Lc-16 Dc-17 Cc-18 Sc-19 Rc-20 Fc-21 Cc-22 Cc-23 Ec-24 Dc-25 Vc-26 Ic-27 Gc-28 Tc-29 Qc-30
Amino Acid – coupling #

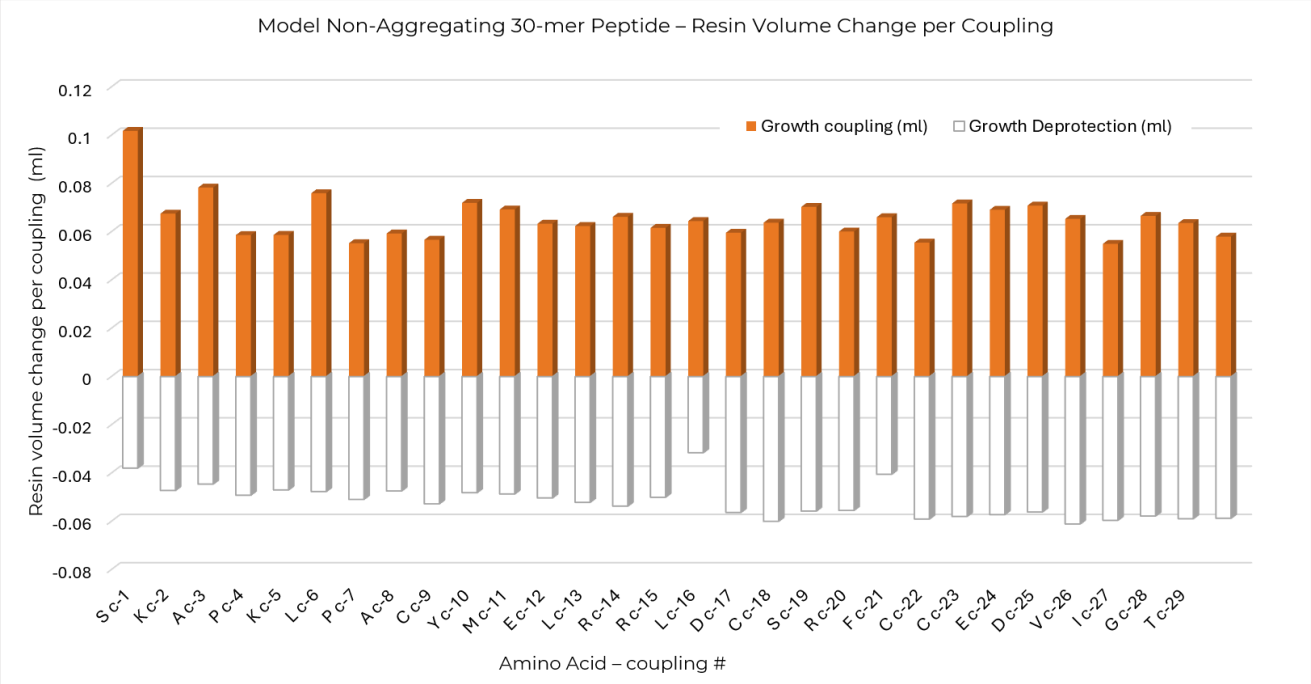
Model Non-Aggregating 30-mer Peptide – Resin Volume Change per Coupling
Growth coupling (ml)
Growth Deprotection (ml)
Resin volume change per coupling (ml)
0.12
0.1
0.08
0.06
0.04
0.02
0
-0.02
-0.04
-0.06
-0.08
Sc-1 Kc-2 Ac-3 Pc-4 Kc-5 Lc-6 Pc-7 Ac-8 Cc-9 Yc-10 Mc-11 Ec-12 Lc-13 Rc-14 Rc-15 Lc-16 Dc-17 Cc-18 Sc-19 Rc-20 Fc-21 Cc-22 Cc-23 Ec-24 Dc-25 Vc-26 Ic-27 Gc-28 Tc-29
Amino Acid – coupling #

JR-10 on TentaGel S

JR-10 [1] is a widely used 10-amino-acid benchmark peptide for evaluating solid-phase peptide synthesis (SPPS). It is regarded as a challenging sequence because its hydrophobic, aggregation-prone nature increases the
likelihood of incomplete couplings and deletion sequences, making it a useful model for comparing peptide synthesis methods.

The cumulative chart shows the onset of aggregation during the coupling of residue 9. The detailed chart provides further insight into this behaviour. Under normal conditions, the peptidyl resin expands during each coupling step and contracts during the subsequent deprotection. At coupling 9, however, the opposite trend is observed: the resin contracts during coupling, indicating aggregation, before recovering during the following deprotection. During coupling 10, the resin contracts further, but in contrast to the previous cycle, no recovery is observed during deprotection. This indicates that the aggregation has become more persistent and is no longer reversed by the deprotection step.

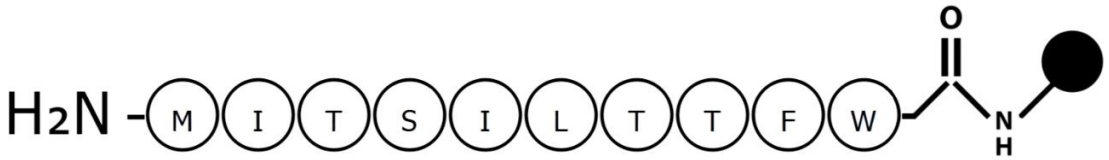

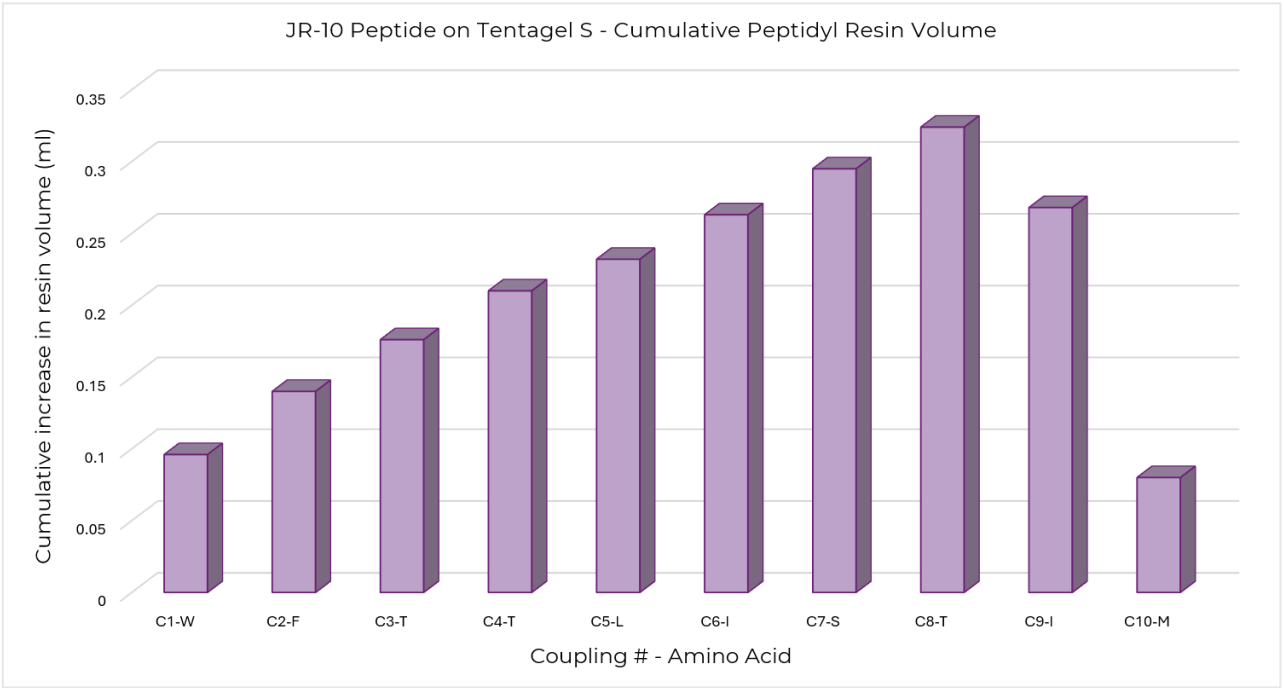

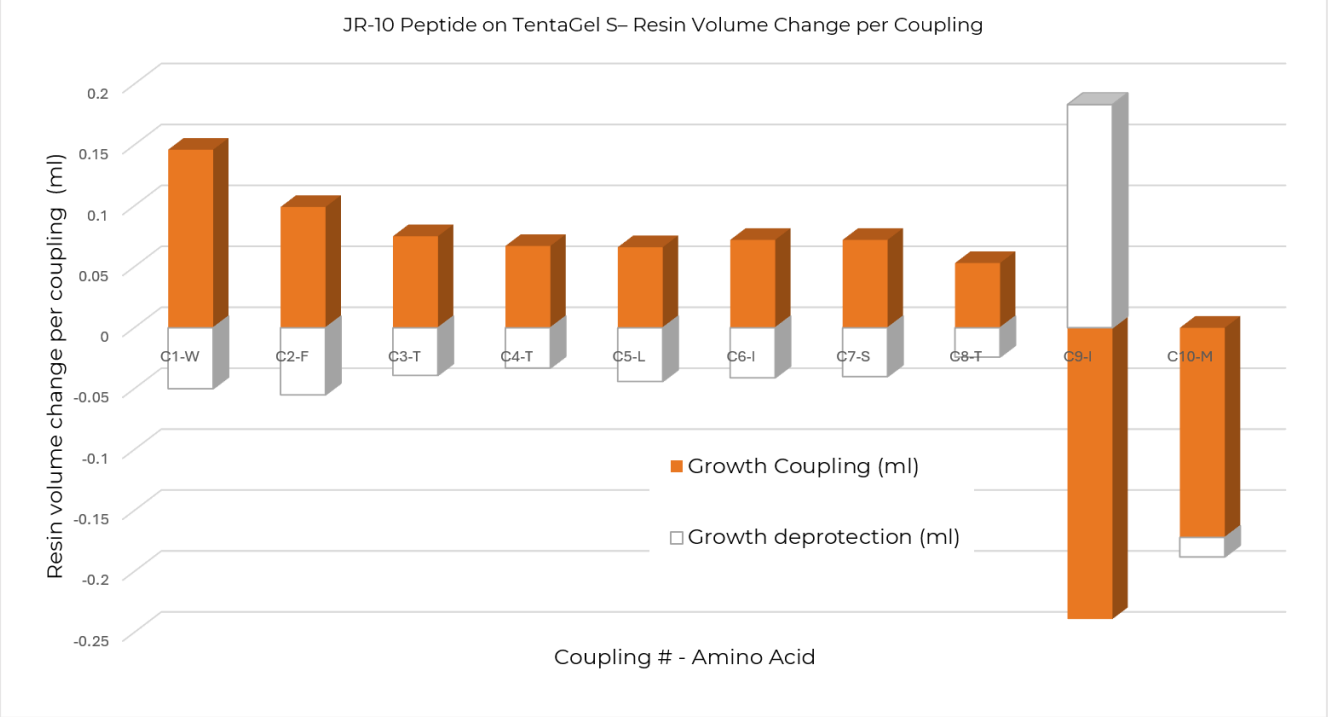

JR-10 on low-loading polystyrene resin

To compare the performance of TentaGel and low-loading polystyrene (PS) resin, the JR-10 peptide was synthesised on both supports. Interestingly, the cumulative aggregation profiles are remarkably similar, showing a minor aggregation event during coupling 9 followed by a more significant aggregation event during coupling 10.

The detailed charts, however, reveal subtle differences in the aggregation behaviour. On PS resin, the aggregation during coupling 9 is less pronounced than on TentaGel, but unlike TentaGel there is no recovery during the subsequent deprotection step. During coupling 10, the behaviour of the two resins is essentially identical, with significant aggregation and no recovery during deprotection.

Overall, these results suggest that changing from TentaGel to low-loading PS resin provides little improvement in the synthesis of the JR-10 peptide, although the mechanism and timing of the initial aggregation event differ slightly between the two supports.

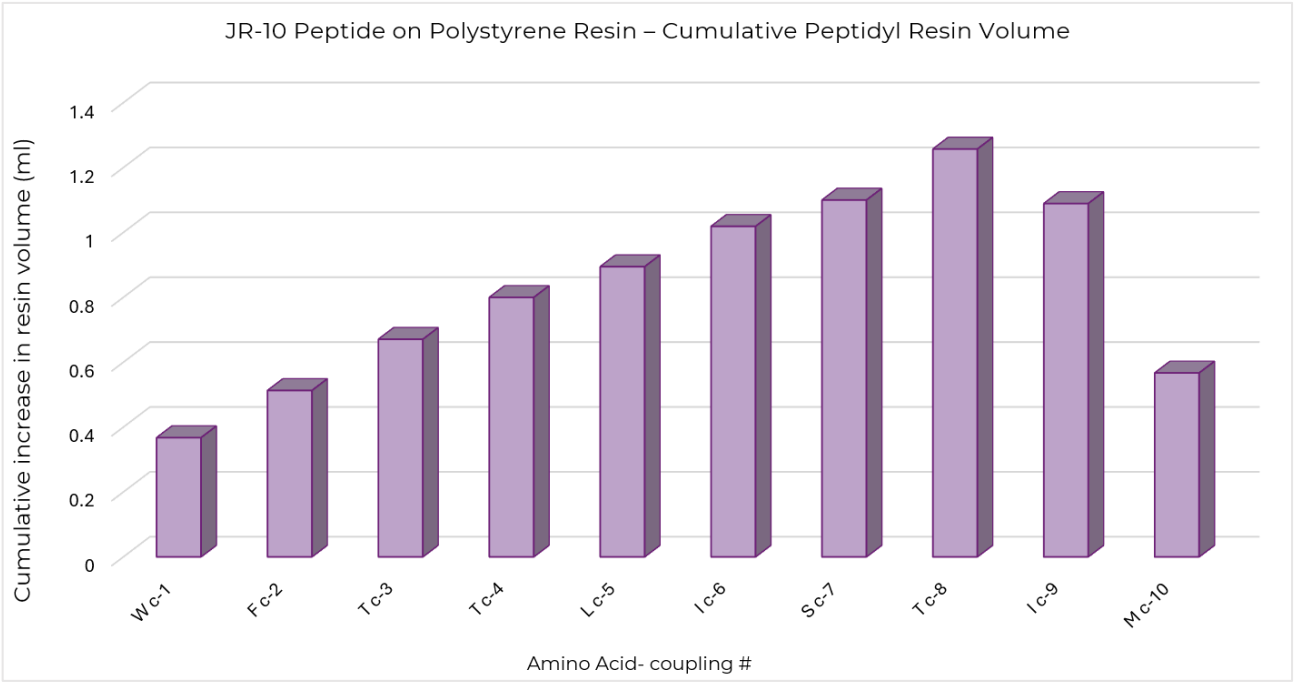
JR-10 Peptide on Polystyrene Resin – Cumulative Peptidyl Resin Volume
Cumulative increase in resin volume (ml)
1.4
1.2
1
0.8
0.6
0.4
0.2
0
Wc-1
Fc-2
Tc-3
Tc-4
Lc-5
Ic-6
Sc-7
Tc-8
Ic-9
Mc-10
Amino Acid- coupling #

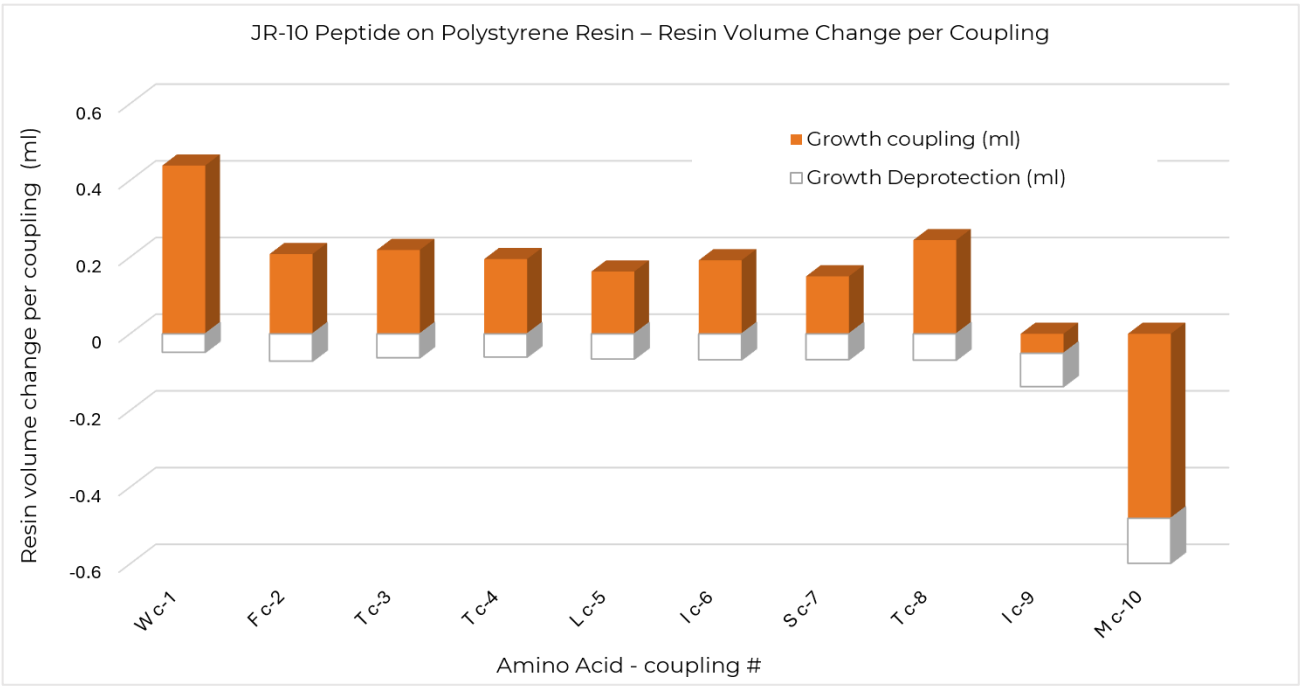
JR-10 Peptide on Polystyrene Resin – Resin Volume Change per Coupling
Resin volume change per coupling (ml)
0.6
0.4
0.2
0
-0.2
-0.4
-0.6
Growth coupling (ml)
Growth Deprotection (ml)
Wc-1
Fc-2
Tc-3
Tc-4
Lc-5
Ic-6
Sc-7
Tc-8
Ic-9
Mc-10
Amino Acid - coupling #

ACP peptide on TentaGel S (all couplings in DMF)

The cumulative chart shows the onset of aggregation during the coupling of residue 10. As with the JR-10 peptide, the detailed chart provides further insight into the aggregation process. The resin contracts during the coupling step, indicating aggregation, before recovering during the subsequent deprotection step. This suggests that the aggregation event is initially reversible under the deprotection conditions.

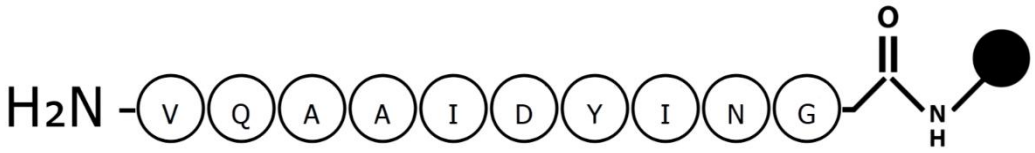

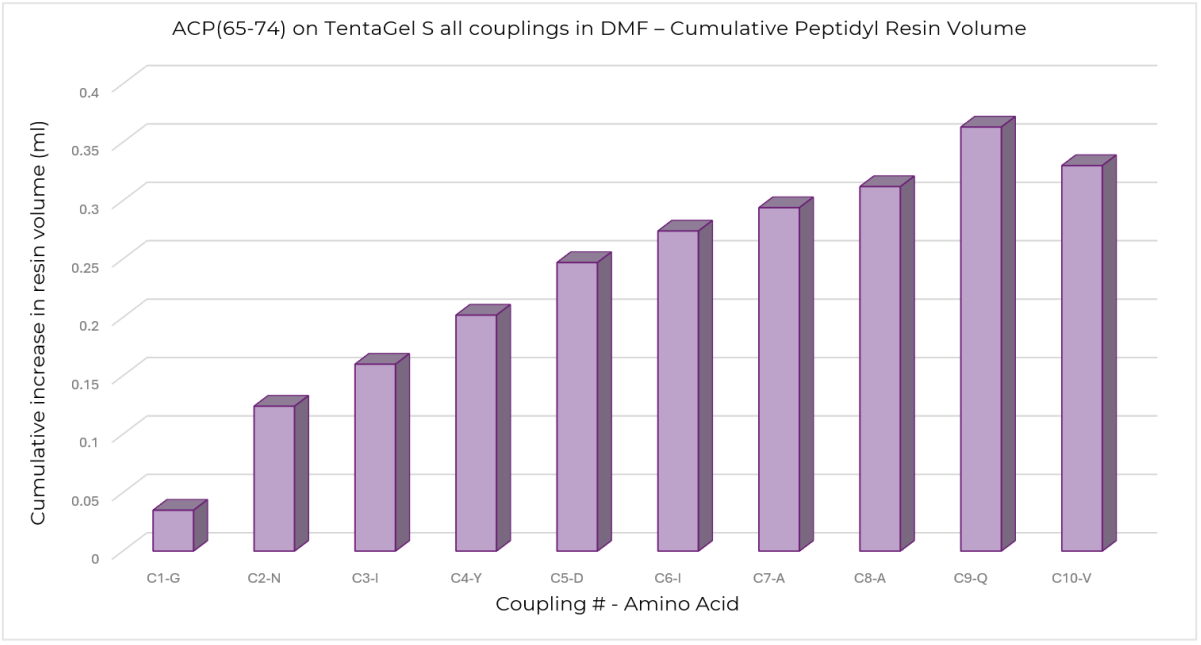

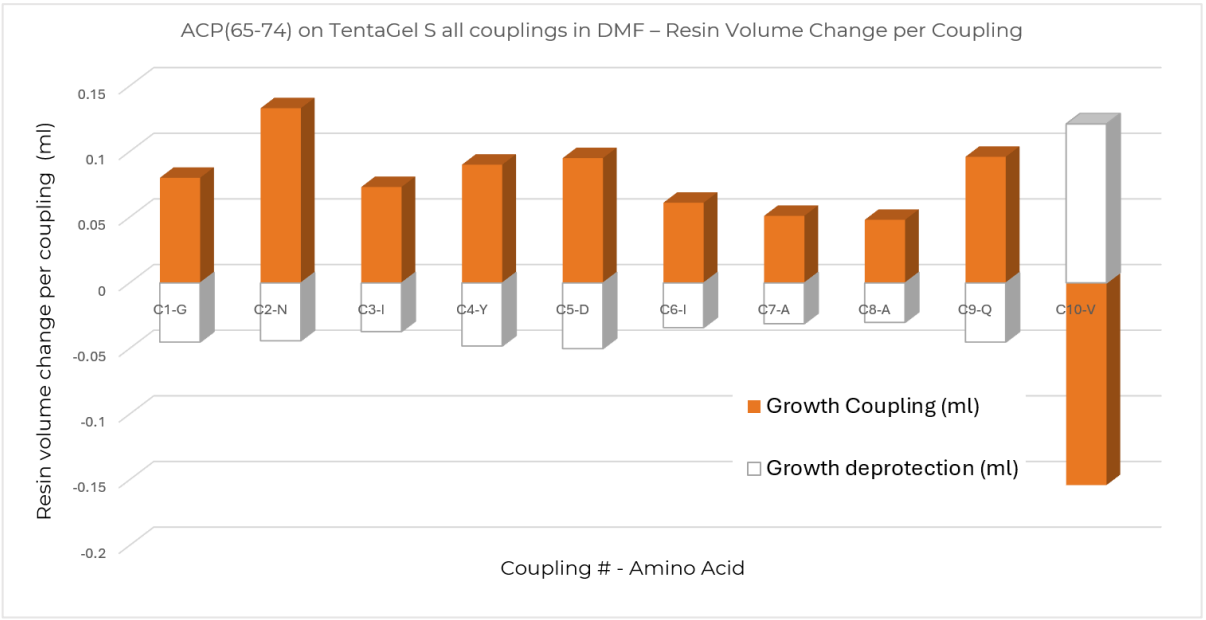

ACP peptide on TentaGel S (DMSO added for the final coupling)

For the ACP peptide [2], it is well documented that performing the 10th coupling in a mixture of DMF and DMSO suppresses aggregation. The two charts below demonstrate this effect. Both the cumulative and detailed charts show that the inclusion of DMSO in the solvent system suppresses aggregation, restoring the regular expansion of the peptidyl resin during coupling and contraction during deprotection characteristic of a non-aggregating synthesis.

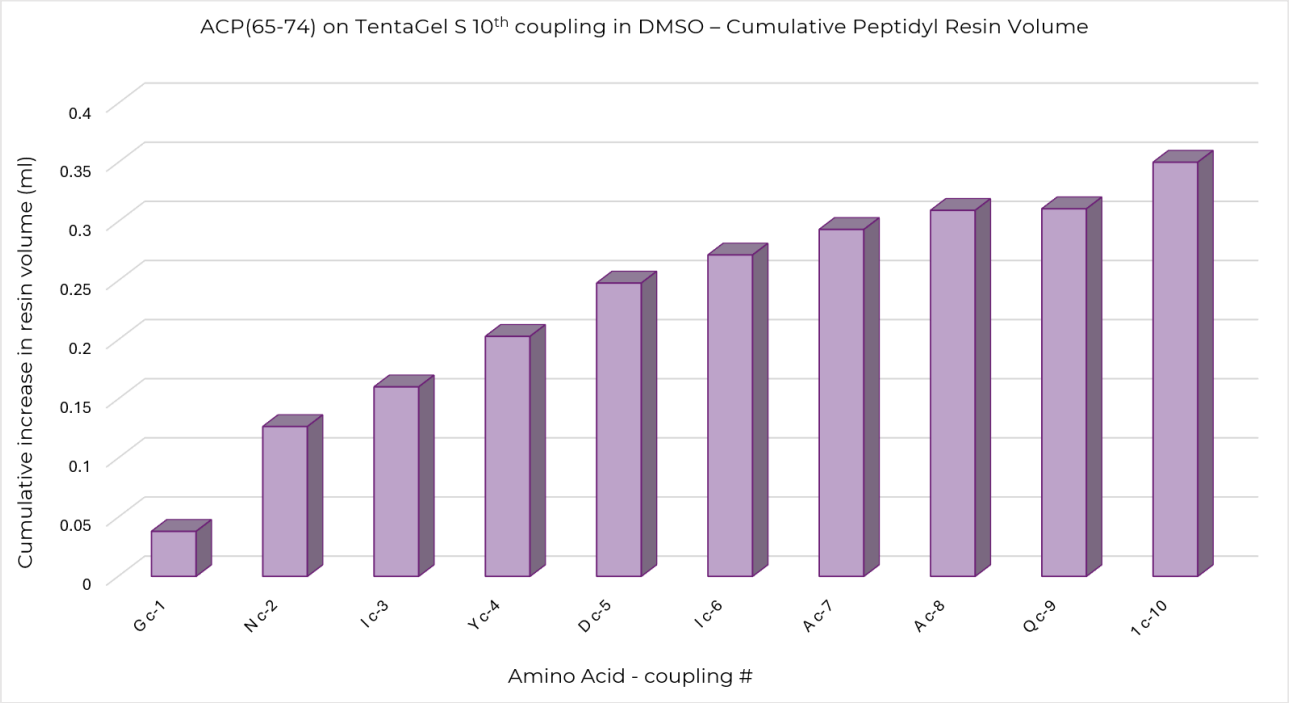

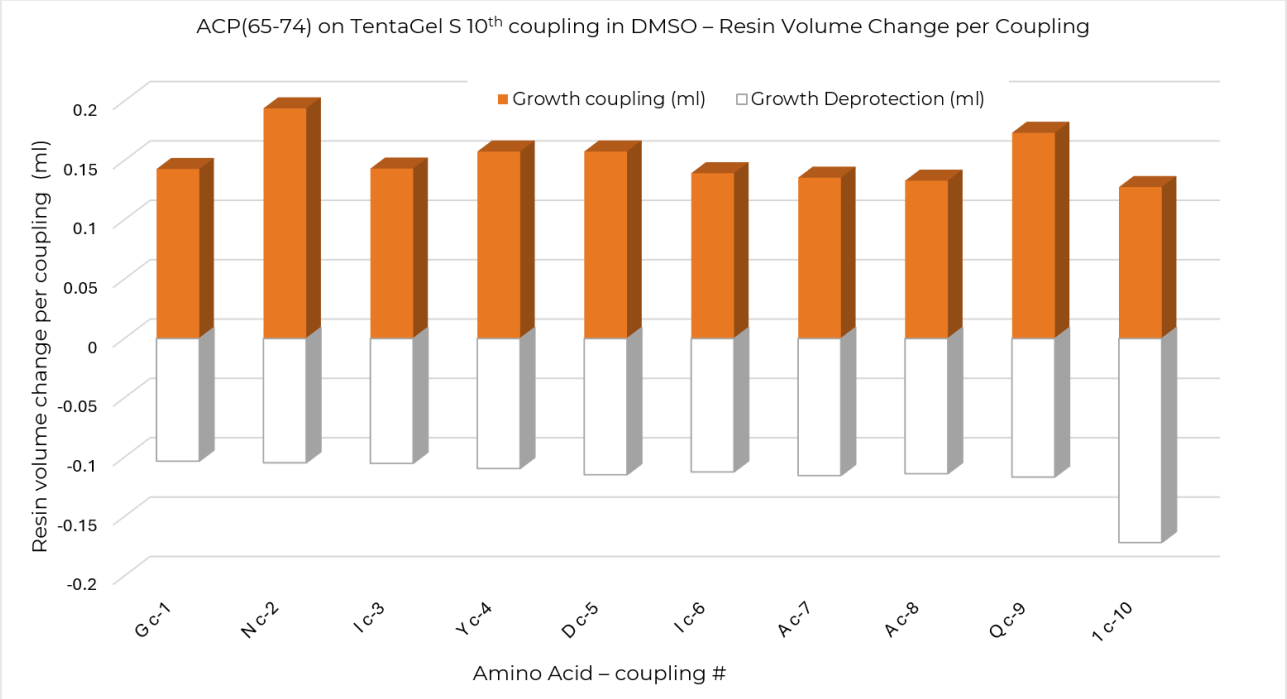

GLP-1 analogue 30-mer on TentaGel S

GLP-1(7–36) [3] amide is the biologically active form of glucagon-like peptide-1, an incretin hormone that stimulates glucose-dependent insulin secretion, suppresses glucagon release, and delays gastric emptying. It forms the basis of a class of highly successful medicines for the treatment of type 2 diabetes and obesity.

Although GLP-1 is known to undergo aggregation during solid-phase peptide synthesis, it is generally considered a relatively straightforward peptide to synthesise. The cumulative chart clearly shows the onset of aggregation during the coupling of residue 10. The detailed chart provides further insight, revealing contraction of the peptidyl resin during the coupling of glutamic acid (E), with no recovery during the subsequent deprotection step. However, from residue 11 onwards the synthesis returns to the characteristic behaviour of a non-aggregating peptide, with resin expansion during coupling followed by contraction during deprotection. This rapid recovery from the aggregation event may explain why GLP-1 can be synthesised efficiently despite the transient aggregation observed during its synthesis.

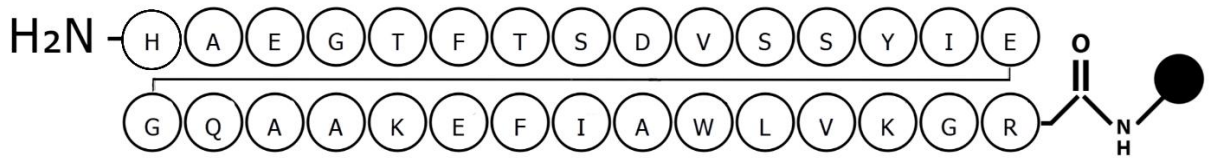

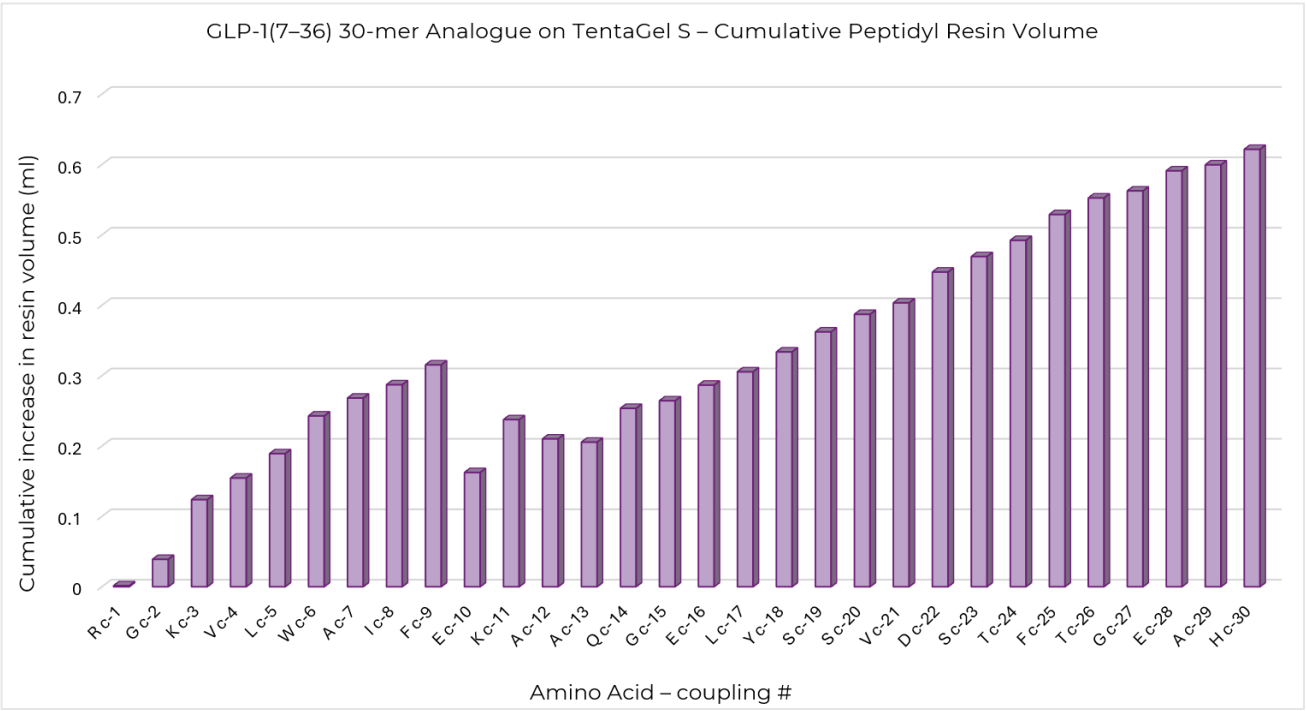

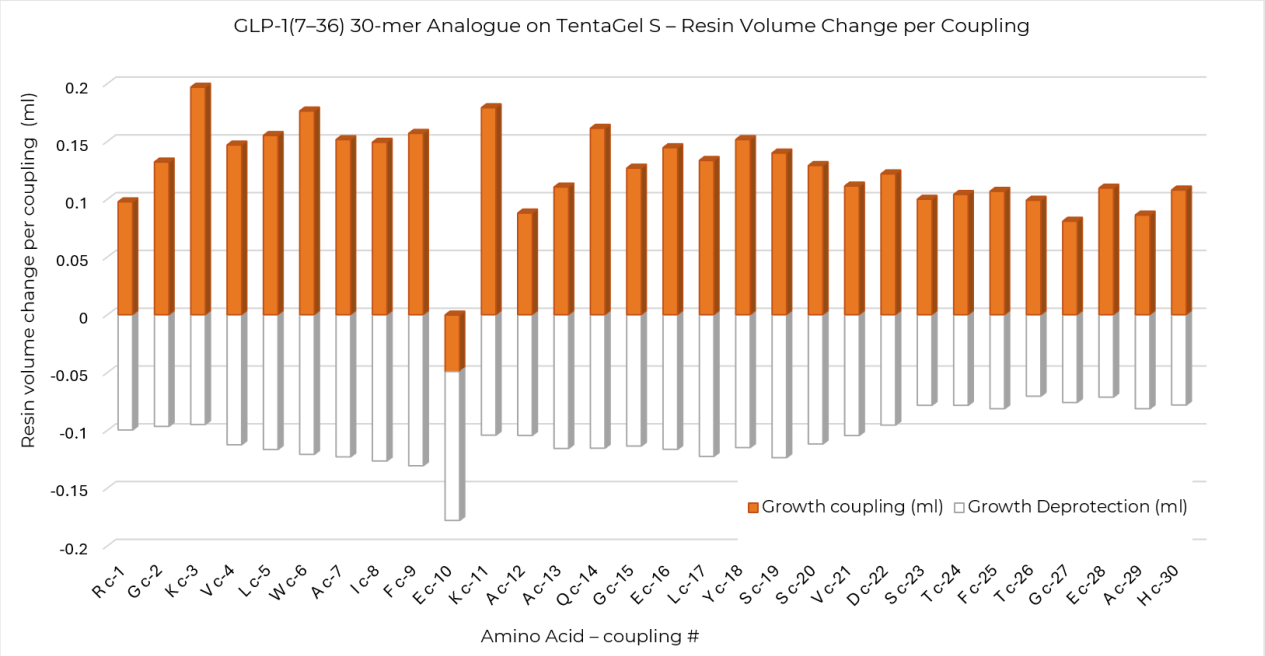

Barstar fragment on TentaGel S

Barstar(61–90) [4] is a 30-amino-acid fragment of the bacterial protein barstar, the natural inhibitor of the ribonuclease barnase. The peptide is widely used as a model in peptide synthesis studies because its length and sequence complexity provide a representative challenge for the preparation of longer peptides while remaining relatively straightforward to characterise.

The cumulative chart shows the onset of severe aggregation during the coupling of residue 7 (D). However, the detailed chart reveals that the synthesis begins to deviate from normal behaviour one coupling earlier. During the coupling of residue 6 (I), the peptidyl resin contracts significantly, indicating aggregation, before fully recovering during the subsequent deprotection step. Couplings 7, 8 and 9 also exhibit abnormal behaviour, with smaller but persistent deviations from the characteristic coupling and deprotection profile of a non-aggregating peptide. It is not until the coupling of residue 10 (E) that the characteristic pattern of a non-aggregating peptide is restored, with consistent resin expansion during coupling followed by contraction during deprotection.

These observations demonstrate that aggregation during the synthesis of Barstar(61–90) is both dynamic and prolonged, rather than a single discrete event. The need for several successive coupling and deprotection cycles before normal resin swelling behaviour is restored helps explain why this peptide often requires extended synthesis protocols to achieve even moderate crude purity.

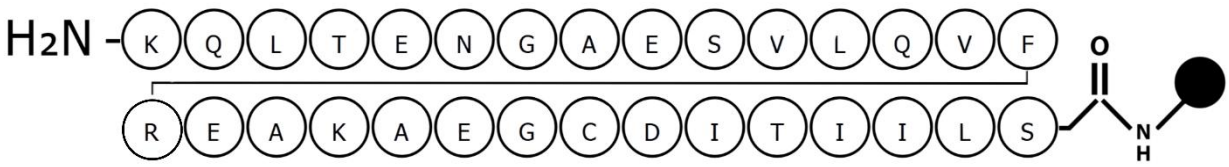

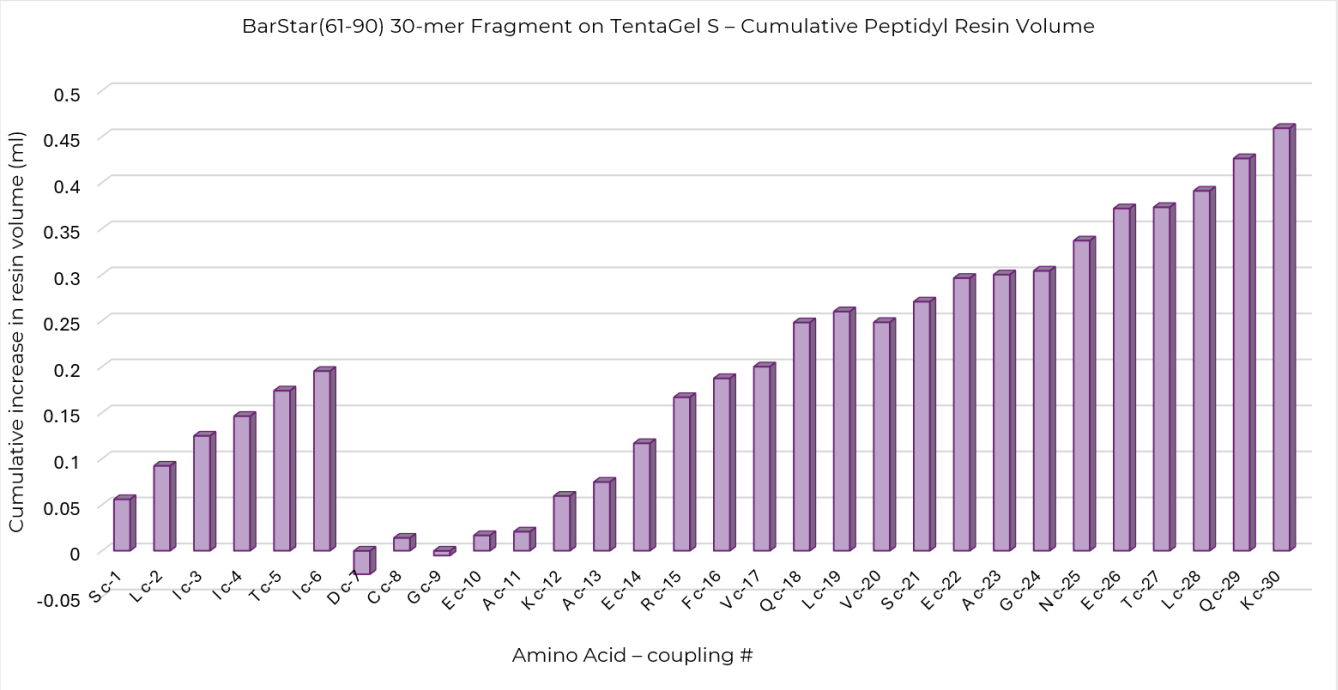
BarStar(61-90) 30-mer Fragment on TentaGel S – Cumulative Peptidyl Resin Volume
Cumulative increase in resin volume (ml)
0.5
0.45
0.4
0.35
0.3
0.25
0.2
0.15
0.1
0.05
0
-0.05
Sc-1 Lc-2 Ic-3 Ic-4 Tc-5 Ic-6 Dc-7 Cc-8 Gc-9 Ec-10 Ac-11 Kc-12 Ac-13 Ec-14 Rc-15 Fc-16 Vc-17 Qc-18 Lc-19 Vc-20 Sc-21 Ec-22 Ac-23 Gc-24 Nc-25 Ec-26 Tc-27 Lc-28 Qc-29 Kc-30
Amino Acid – coupling #

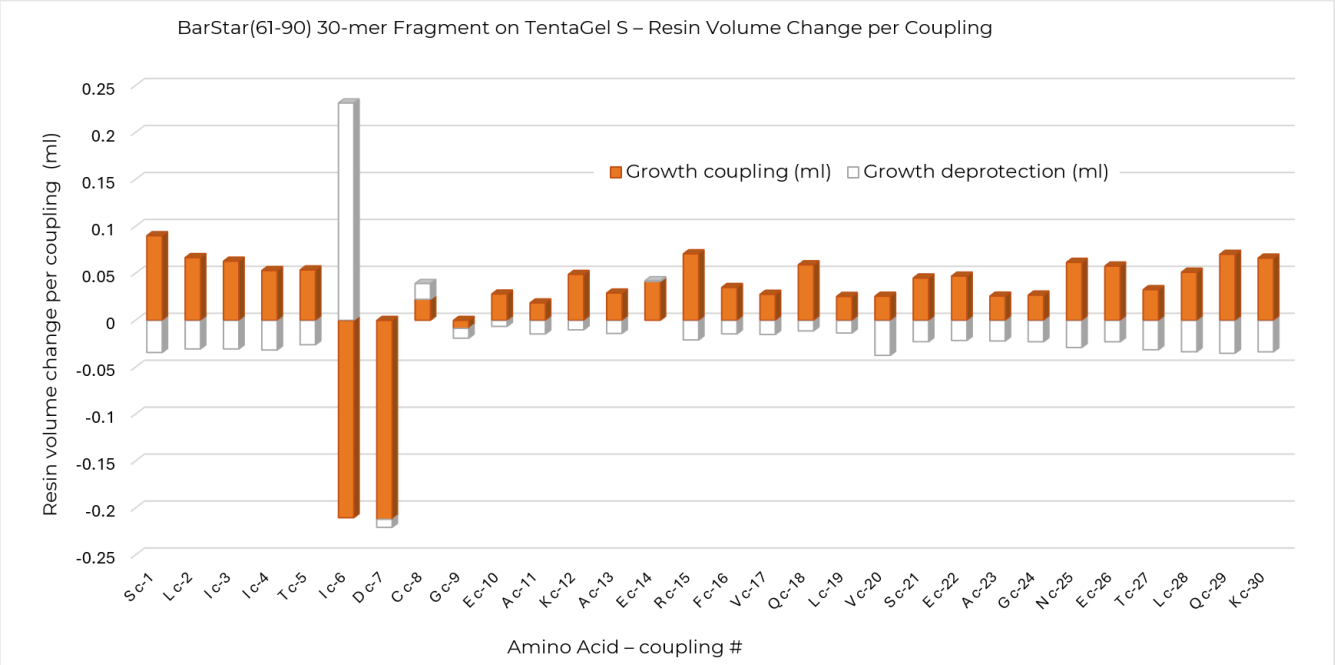
BarStar(61-90) 30-mer Fragment on TentaGel S – Resin Volume Change per Coupling
Resin volume change per coupling (ml)
Growth coupling (ml)
Growth deprotection (ml)
0.25
0.2
0.15
0.1
0.05
0
-0.05
-0.1
-0.15
-0.2
-0.25
Sc-1 Lc-2 Ic-3 Ic-4 Tc-5 Ic-6 Dc-7 Cc-8 Gc-9 Ec-10 Ac-11 Kc-12 Ac-13 Ec-14 Rc-15 Fc-16 Vc-17 Qc-18 Lc-19 Vc-20 Sc-21 Ec-22 Ac-23 Gc-24 Nc-25 Ec-26 Tc-27 Lc-28 Qc-29 Kc-30
Amino Acid – coupling #

Conclusion

The examples presented in this application note demonstrate that real-time monitoring of resin volume using Vapourtec's patented VBFR™ technology provides a simple and effective means of identifying peptide aggregation during SPPS. Rather than inferring aggregation from poor crude purity or reduced coupling efficiency after synthesis is complete, aggregation events can be observed directly, localized to individual amino acid residues, and monitored as they evolve throughout the synthesis.

This capability provides valuable insight during peptide method development. By identifying not only where aggregation begins, but also whether it is transient, persistent or reversible, chemists can make more informed decisions when selecting optimisation strategies. These may include increasing coupling or deprotection times, raising reaction temperature, introducing backbone-modified amino acids such as pseudoproline dipeptides, or adjusting solvent and reagent conditions only where required. This targeted approach can improve peptide purity while avoiding unnecessary increases in synthesis time and reagent consumption.

Beyond method development, VBFR™ analysis provides a powerful process analytical tool for comparing synthesis strategies, evaluating challenging peptide sequences and increasing confidence during process scale-up. By transforming changes in peptidyl resin volume into meaningful process information, the Peptide-Builder™ provides peptide chemists with a unique real-time view of peptide synthesis that is not available using conventional peptide synthesizers.

References

1. JR-10 aggregation - Jonathan M. Collins, Keith A. Porter, Sandeep K. Singh, Grace S. Vanier; High-Efficiency Solid Phase Peptide Synthesis (*HE*-SPPS). *Org. Lett.* 7 February 2014; 16 (3): 940–943. https://doi.org/10.1021/ol4036825

2. ACP aggregation – S. J. Paravizzini, L. M. Haugaard-Kedström, C. A. Hutton, J. A. Karas, *Angew. Chem. Int. Ed.* 2025, 64, e202509939. https://doi.org/10.1002/anie.202509939

3. GLP-1 aggregation - Somesh Mohapatra, Nina Hartrampf, Mackenzie Poskus, Andrei Loas, Rafael Gómez-Bombarelli, Bradley L. Pentelute; Deep Learning for Prediction and Optimization of Fast-Flow Peptide Synthesis. *ACS Cent. Sci.* 23 December 2020; 6 (12): 2277–2286. https://doi.org/10.1021/acscentsci.0c00979

4. Barstar aggregation - Héloïse Bürgisser, Elyse T. Williams, Aliénor Jeandin, Robin Lescure, Adhvitha Premanand, Songlin Wang, Nina Hartrampf; A Versatile “Synthesis Tag” (SynTag) for the Chemical Synthesis of Aggregating Peptides and Proteins. *Journal American Chemical Society* 18 December 2024; 146 (50): 34887–34899. https://doi.org/10.1021/jacs.4c14247